Electronic Structure of Bis(*o*-iminobenzosemiquinonato)metal Complexes (Cu, Ni, Pd). The Art of Establishing Physical Oxidation States in Transition-Metal Complexes Containing Radical Ligands

Phalguni Chaudhuri,* Claudio Nazari Verani, Eckhard Bill, Eberhard Bothe, Thomas Weyhermüller, and Karl Wieghardt*

Contribution from the Max-Planck-Institut für Strahlenchemie, Stiftstrasse 34-36, D-45470 Mülheim an der Ruhr, Germany

Received October 31, 2000

Abstract: The ligand 2-anilino-4,6-di-*tert*-butylphenol and its 2-(3,5-dichloroanilino)-4,6-di-*tert*-butylphenol analogue react in CH_3CN or CH_3OH solutions with divalent transition metal ions in the presence of air and triethylamine. Depending on the metal:ligand ratio (1:1, 1:2, or 1:3) and the presence (or absence) of the cyclic amine 1,4-dimethyl-1,4,7-triazacyclononane (dmtacn), the following complexes have been isolated as crystalline solids: $[Co^{III}(L^{ISQ})_3]$ (**1**); $[Cu^{II}(dmtacn)(L^{ISQ})]PF_6$ (**2**); $[Cu^{II}(L^{ISQ})_2]$ (**3**); $[Ni^{II}(L^{ISQ})_2]$ (**4a**); $[Ni^{II}(^{Cl}L^{ISQ})_2]$ (**4b**); $[Pd^{II}(L^{ISQ})_2]$ (**5**). $(L^{ISQ})^-$ represents the monoanionic *o*-iminobenzosemiquinonate radical ($S_{rad} = {}^1/_2$). Compounds **1**−**5** have been characterized by single-crystal X-ray crystallography at 100(2) K. For all complexes it is unambiguously established that the O,N-coordinated *o*-iminobenzosemiquinonato(1−) ligand is present. Complexes **3**, **4b**, and **5** are square planar molecules which possess an $S_t = {}^1/_2$, 0, and 0 ground state, respectively, as was established by ^1H NMR and EPR spectroscopies and variable-temperature magnetic susceptibility measurements. Complex **2** possesses an $S_t = 1$ ground state which is attained via strong intramolecular ferromagnetic coupling ($J = +195$ cm^{-1}) between the $d_{x^2-y^2}$ magnetic orbital of the Cu^{II} ion and the π-orbital of the ligand radical. Complex **1** contains three mutually orthogonal $(L^{ISQ})^{-\bullet}$ ligands and has an $S_t = {}^3/_2$ ground state. It is shown that the electronic structure of **4a** and **5** is adequately described as singlet diradical containing a divalent, diamagnetic d^8 configured central metal ion and two strongly antiferromagnetically coupled $(L^{ISQ})^-$ radical ligands. It is concluded that the same electronic structure prevails in the classic bis(*o*-diiminobenzosemiquinonato)- and bis(*o*-benzosemiquinonato)metal complexes of Ni^{II}, Pd^{II}, and Pt^{II}. The electrochemistry of all complexes has been investigated in detail. For **3**, **4a**, and **5** a series of reversible one-electron-transfer waves leads to the formation of the anions and cations $[M(L)_2]^{2-,1-,1+,2+}$ which have been characterized spectroelectrochemically. All redox processes are shown to be ligand-based.

Introduction

The *formal* oxidation number (state) of a given metal ion in a mononuclear coordination compound is a nonmeasurable integer which is commonly defined as "the charge left on the metal after all ligands have been removed in their normal, closed-shell configuration−that is with their electron pair".[1]

In contrast, it is accepted practice that referring to e.g. an iron(III) complex implies that this compound contains an iron ion with a d^5 high-, intermediate-, or low-spin electron configuration. Since *n* for a d^n electronic configuration is, at least, in principle, a measurable quantity (by various spectroscopies), Jörgensen has suggested[2] that an oxidation number which is derived from a known d^n configuration should be specified as *physical* (or *spectroscopic*) oxidation number (state).

In many cases *formal* and *spectroscopic* oxidation numbers are *identical* as is exemplified for $[Co(NH_3)_6]^{3+}$ where the low-spin d^6 cobalt ion possesses a +III oxidation state, both formally and physically. This is not necessarily always the case.

Discrepancies arise when organic radicals with an open-shell electron configuration are coordinated to a transition metal ion. For example, consider an O-coordinated phenoxyl radical complex of an iron ion with a d^5 configuration, Fe(III)−Ȯ−Ph. According to the above definition the *formal* oxidation number for the iron ion would have to be +IV since a closed-shell phenolato anion would have to be removed. On the other hand, Mössbauer and resonance Raman spectroscopies unequivocally prove the presence of a high-spin d^5 electron configuration at the metal ion and of a phenoxyl ligand, respectively.[3] Thus the iron ion has a physical oxidation number of +III. We clearly understand that an Fe(IV)−phenolato complex has a distinctly different electronic structure than an Fe(III)−phenoxyl species.

Since the term physical (or spectroscopic) oxidation state is not accepted by the community, both *formal* and *physical* oxidation numbers are often used (and understood) as synonyms−which they are not. In some areas of coordination chemistry this practice, unfortunately, leads to considerable confusion. In contrast, the terms *innocent* and *noninnocent* ligands are widely used to emphasize the fact that some ligands do not necessarily possess a closed-shell configuration. These terms can only be

(1) Hegedus, L. S. In *Transition Metals in the Synthesis of Complex Organic Molecules*; University Science Books: Mill Valley, CA, 1994; p 3.

(2) Jörgensen, C. K. In *Oxidation Numbers and Oxidation States*; Springer: Heidelberg, Germany, 1969.

(3) Snodin, M. D.; Ould-Moussa, L.; Wallmann, U.; Lecomte, S.; Bachler, V.; Bill, E.; Hummel, H.; Weyhermüller, T.; Hildebrandt, P.; Wieghardt, K. *Chem. Eur. J.* **1999**, *5*, 2554.

used meaningfully in conjunction with the *physical* oxidation state of the metal ion.

In this paper we address a problem which has been discussed controversially in the literature for more than four decades.[4,5] Consider the complexes A[6,7] and B;[8] both compounds have been synthesized and are structurally characterized.[6−11] They are planar molecules and diamagnetic ($S = 0$) in the solid state and in solution. What are the physical oxidation states of the
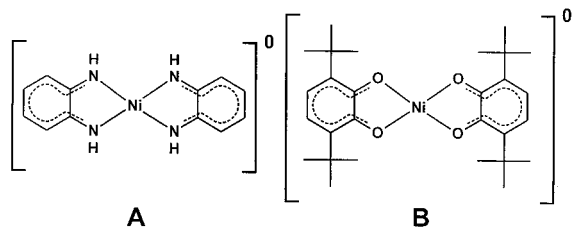
central nickel ion and of the ligands? What is their electronic structure and how should we describe it?

Two extremes have been seriously considered after higher physical oxidation states than +II for the nickel ions have been refuted:[7] (i) Gray et al.[7] proposed that the Ni^{II}, d^8, complex A should be understood as a diradical with a singlet ground state as shown in C. (ii) Holm et al.[4,6] felt that the two resonance hybrids of structure D adequately describe the ground state. On the basis of structural data, Abakumov et al.[8] and Pierpont et al.[8,10] have assigned an electronic structure for B and its Pd
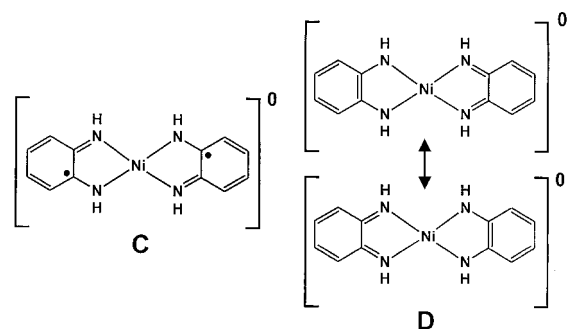

and Pt analogues, which is derived from two intramolecularly antiferromagnetically coupled benzosemiquinonato(1−) ligands. These complexes are thus also considered to be singlet diradicals. In the past it has been inferred that the description of the electronic structure as singlet diradical is equivalent to an orbital description in which the HOMO contains two paired electrons, whose distribution is such as to afford ligand geometry structures corresponding to two radicals. This is not the case. A HOMO occupied by two electrons of opposite spin implies that both electrons occupy the same regions of space in a molecule and,

(4) (a) Holm, R. H.; O'Connor, M. J. *Prog. Inorg. Chem.* **1971**, *14*, 241. (b) Forbes, C. E.; Gold, A.; Holm, R. H. *Inorg. Chem.* **1971**, *10*, 2479.

(5) (a) Pierpont, C. G.; Lange, C. W. *Prog. Inorg. Chem.* **1994**, *41*, 331. (b) Speier, G.; Whalen, A. M.; Csihony, J.; Pierpont, C. G. *Inorg. Chem.* **1995**, *34*, 1355. (c) Whalen, A. M.; Bhattacharya, S.; Pierpont, C. G. *Inorg. Chem.* **1994**, *33*, 347.

(6) Balch, A. L.; Holm, R. H. *J. Am. Chem. Soc.* **1966**, *88*, 5201.

(7) Stiefel, E. I.; Waters, J. H.; Billig, E.; Gray, H. B. *J. Am. Chem. Soc.* **1965**, *87*, 3016.

(8) (a) Abakumov, G. A.; Cherkasov, V. K.; Bubnov, M. P.; Ellert, O. G.; Rakitin, Y. V.; Zakharov, L. N.; Struchkov, Y. T.; Saf'yanov, Y. N. *Bull. Russ. Acad. Sci.* **1992**, *41*, 1813. Translated from: *Izv. Akad. Nauk, Ser. Khim.* **1992**, *10*, 2315. (b) Lange, C. W.; Pierpont, C. G. *Inorg. Chim. Acta* **1997**, *263*, 219.

(9) Swartz Hall, G.; Soderberg, R. H. *Inorg. Chem.* **1968**, *11*, 2300.

(10) Fox, G. A.; Pierpont, C. G. *Inorg. Chem.* **1992**, *31*, 3718.

(11) Mederos, A.; Dominguez, S.; Hernández-Molina, R.; Sanchiz, J.; Brito, F. *Coord. Chem. Rev.* **1999**, *193−195*, 913.

Scheme 1. Ligands and Complexes Prepared and Labels

Ligands:
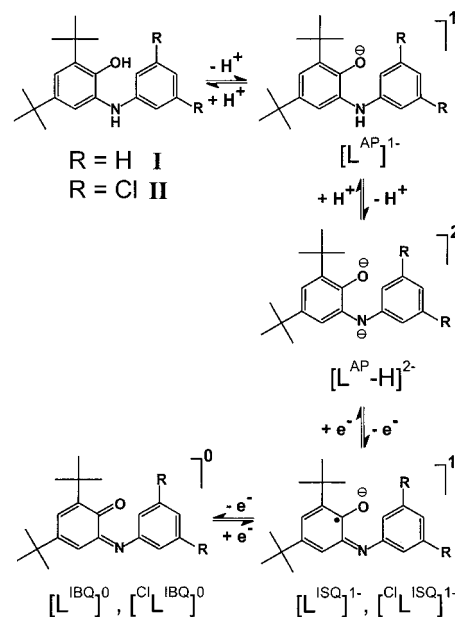
Complexes:

therefore, double occupation of this HOMO *forces* the two electrons to come close to each other which immediately implies a *strong* antiferromagnetic coupling. A singlet diradical, however, is characterized by two electrons, which can be weakly antiferromagnetically coupled. The correct wave function must, therefore, have the flexibility that these two electrons of opposite spin have the option to avoid each other in space. In other words, even for a qualitative description of a singlet diradical, a procedure comprising electron correlation is mandatory. A double occupation of a HOMO clearly excludes this essential correlation.

Since the energies of the electronic structures represented in C and D are different, the question what the ground state of A and B actually is, is a physical, one which should be amenable to experiment. We decided to investigate the coordination chemistry of a ligand which represents a hybrid between the above *o*-phenylenediamine and catecholate derivatives and employed the *N*-phenyl-*o*-aminophenols **I** and **II** shown in Scheme 1. These ligands can coordinate in their singly and doubly deprotonated forms, (L^{AP})$^-$ and (L^{AP}-H)$^{2-}$, in an O,N-bidentate fashion. They can also be oxidized to the *o*-iminobenzosemiquinonate monoanions, (L^{ISQ})$^-$ and (^{Cl}L^{ISQ})$^-$, which are radicals ($S_{rad} = ^1/_2$) and, finally, they can form the neutral bidentate *o*-iminobenzoquinone ligands (L^{IBQ}) and (^{Cl}L^{IBQ}). Exactly the same chemistry is known for *o*-catecholates[5] and *o*-phenylenediamines.[11]

The actual oxidation level of the latter coordinated ligands can be determined from high-quality X-ray structure determinations. It is well established that the C−O, C−N, and C−C distances vary in a systematic fashion in coordinated *o*-catecholates(2−), *o*-benzosemiquinonates(1−), and benzo-

quinones or *o*-phenylenediamido(2−), *o*-diiminobenzosemi-quinonates(1−), or *o*-diiminobenzoquinones.[5,11] For simple *o*-aminophenolates this has not been established previously although some coordination chemistry of rather similar *tert*-butyl-substituted phenoxazinolate semiquinone radicals has been described by Pierpont and co-workers.[5b,c]

We describe here a series of complexes containing one, two, or three O,N-coordinated *o*-iminobenzosemiquinonato(1−) ligands (Scheme 1). We present evidence that the neutral, square planar complexes $[M^{II}(L^{ISQ})_2]$ (M^{II} = Cu, Ni, Pd) and analogous complexes of type A and B are diradicals with a singlet ground state.

Experimental Section

The synthesis of the ligand 1,4-dimethyl-1,4,7-triazacyclononane (dmtacn) was performed according to a literature procedure.[13]

Preparation of the Ligands I and II. 2-Anilino-4,6-di-*tert*-butylphenol (**I**) and 2-(3,5-dichloroanilino)-4,6-di-*tert*-butylphenol (**II**) were prepared according to a slightly modified procedure described in ref 12.

To a solution of 3,5-di-*tert*-butylcatechol (10 g; 45 mmol) and triethylamine (0.6 mL) in *n*-heptane (30 mL) was added dropwise a solution of aniline or 3,5-dichloroaniline (45 mmol) in *n*-heptane (15 mL). The resulting mixture was heated to reflux for 5 h. The suspension was stored at 4 °C for 12 h after which time a white (brownish) solid was collected by filtration, washed with cold *n*-heptane, and air-dried. The compounds were recrystallized from *n*-hexane yielding colorless crystalline materials. The yields were in both cases 80−85% based on the starting catechol. ^{1}H NMR (400 MHz, 300 K): **I** (CD_2Cl_2), δ = 1.28 (s, 9H), 1.46 (s, 9H), 4.99 (s, 1H), 6.3−7.05 (arom. H, 7H), mp 145−147 °C; **II** (CH_3OH), δ = 1.27 (s, 9H), 1.42 (s, 9H), 4.58 (1H), 6.5−7.2 (arom. protons, 5H). ^{13}C {^{1}H} NMR (100.6 MHz): **I** ($CDCl_3$), δ = 29.52, 31.38, 34.35, 34.98, 115.0, 119.76, 121.49, 121.97, 127.73, 129.31, 135.28, 142.18, 146.78, 149.37; **II** (CH_3OH), δ = 30.11, 32.02, 35.17, 36.04, 113.58, 118.25, 122.16, 122.48, 128.81, 136.35, 137.75, 143.22, 150.34, 151.29. EI mass spectrum for **I** and **II**: m/z = 297 [M[+]] and 365 [M − H][+], respectively. Anal. Calcd for $C_{20}H_{27}NO$: C, 80.76; H, 9.15; N, 4.71. Found: C, 80.4; H, 8.9; N, 4.5. To obtain the electronic spectrum of the *o*-iminobenzoquinone derivative of **I** we have oxidized **I** in CH_2Cl_2 solution (1×10^{-4} M) with an excess of Pb(acetate)$_4$ (5×10^{-4} M) at ambient temperature. The electronic spectrum displays absorption maxima at λ = 290 (sh) nm (ϵ = 5.8 × 10^{3} M^{−1} cm^{−1}), 396 (4.8 × 10^{3}), and 488 sh (2.7 × 10^{3}).

Preparation of Complexes. $[Co^{III}(L^{ISQ})_3]$ (1). To a solution of the ligand **I** (0.89 g; 3.0 mmol) in acetonitrile (30 mL) was added anhydrous $Co^{II}Cl_2$ (0.13 g; 1.0 mmol) and triethylamine (1.0 mL). The resulting dark green solution was heated to reflux in the presence of air for 1 h. Slow evaporation of the solvent within 2−3 d at ambient temperature from the solution afforded deep brown crystals of **1**. Yield: 0.61 g (65%). Anal. Calcd for $C_{60}H_{75}N_3O_3Co$: C, 76.24; H, 7.99; N, 4.45; Co, 6.23. Found: C, 76.1; H, 7.9; N, 4.3; Co, 6.3.

$[Cu^{II}(dmtacn)(L^{ISQ})]PF_6$ (2). A methanol solution (30 mL) of $CuCl_2\cdot6H_2O$ (0.170 g; 1.0 mmol) and 1,4-dimethyl-1,4,7-triazacyclononane (0.156 g; 1.0 mmol) was stirred for 30 min at 20 °C after which time the ligand **I** (0.3 g; 1.0 mmol) and NEt$_3$ (0.5 mL) were added in the presence of air. The color of the solution changed to dark green (almost black). The solution was heated to ~60 °C for 1 h. Addition of tetra-*n*-butylammonium hexafluorophosphate (1.94 g; 5 mmol) initiated the precipitation of dark green crystals of **2** within 2−3 d. Yield: ~30%. Anal. Calcd for $C_{28}H_{44}CuF_6N_4OP$: C, 50.86; H, 6.71; N, 8.47; Cu, 9.61. Found: C, 51.1; H, 6.7; N, 8.5; Cu, 9.7. Electrospray mass spectrum (ESI) (CH_3OH, positive ion): m/z = 515.3 {$[Cu^{II}(dmtacn)-(L^{ISQ})]^+$}.

$[Cu^{II}(L^{ISQ})_2]$ (3). To a solution of the ligand **I** (0.59 g; 2.0 mmol) in acetonitrile (30 mL) was added at 40 °C a solid sample of anhydrous Cu^ICl (0.10 g; 1.0 mmol). Upon addition of 0.5 mL of NEt$_3$ in the presence of air the color of the solution changed to green. After heating of the solution for 2 h to reflux, a dark green microcrystalline product of **3** formed upon cooling which was collected by filtration. Yield: 0.55 g (84%). EI mass spectrum: m/z = 653 {M − H}[+] (100%) {M[+]}. Anal. Calcd for $C_{40}H_{50}N_2O_2Cu$: C, 73.41; H, 7.70; N, 4.28; Cu, 9.71. Found: C, 73.3; H, 7.6; N, 4.2; Cu, 9.8.

$[Ni^{II}(L^{ISQ})_2]$ (4a) and $[Ni^{II}(^{Cl}L^{ISQ})_2]$ (4b). Both compounds were obtained by using the same procedure: To a solution of the ligand **I** or **II** (2.0 mmol) in acetonitrile (30 mL) or methanol (30 mL) was added Ni(NO$_3$)$_2\cdot6H_2O$ (0.291 g; 1.0 mmol) and 0.5 mL of NEt$_3$. The solution was heated to reflux in the presence of air for 1 h. Upon cooling, dark green precipitates of **4a** or **4b** formed in ~80% yield. The complexes were recrystallized from a diethyl ether/methanol (3:1) mixture. Anal. Calcd for $C_{40}H_{50}N_2O_2Ni$ (**4a**): C, 73.97; H, 7.76; N, 4.31; Ni, 9.04. Found: C, 73.9; H, 7.7; N, 4.3; Ni, 9.0. Calcd for $C_{40}H_{46}Cl_4N_2O_2Ni$ (**4b**): C, 61.02; H, 5.89; N, 3.56. Found: C, 60.9, H, 6.1; N, 3.3. ^{1}H NMR (400 MHz, $CDCl_3$) of **4a**: δ = 1.03 (s, 18H), 1.06 (s, 18H), 6.46 (d, 2H), 6.88 (d, 2H), 7.38−7.55 (m, 10H). EI-MS of **4a**: m/z = 648 {M − H}[+] (100%).

$[Pd^{II}(L^{ISQ})_2]$ (5). To a solution of the ligand **I** (0.59 g; 2.0 mmol) in acetonitrile (50 mL) was added anhydrous $PdCl_2$ (0.177 g; 1.0 mmol) and 0.5 mL of NEt$_3$ under an argon-blanketing atmosphere. The solution was stirred at 20 °C for 30 min. and then heated to reflux for 20 min. The solution was then exposed to air and stirred for 3−4 h at ambient temperature. After storage of the solution at 0 °C for ~12 h the green precipitate of **5** was collected by filtration. Recrystallization from CH_3CN solution afforded X-ray-quality crystals. Yield: 0.4 g (60%). Anal. Calcd for $C_{40}H_{50}N_2O_2Pd$: C, 68.90; H, 7.23; N, 4.02, Pd, 15.26. Found: C, 68.2; H, 7.2; N, 4.3; Pd, 15.0. EI mass spectrum: m/z = 696 {M − H}[+] (100%). ^{1}H NMR (400 MHz, $CDCl_3$): δ = 1.12 (s, 18H), 1.14 (s, 18H), 6.60 (d, 2H), 6.8 (br, 2H), 7.40−7.42 (m, 10H).

Physical Measurements. Electronic spectra of the complexes and spectra of the spectroelectrochemical investigations were recorded on a HP 8452A diode array spectrophotometer (range: 221−1100 nm). Cyclic voltammograms, square-wave voltammograms, and coulometric experiments were performed using an EG & G potentiostat/galvanostat. Simulations of the cyclic voltammograms were obtained using the program DigiSim 3.0 (Bioanalytical Systems, Inc., West Lafayette, IN). Temperature-dependent (2−298 K) magnetization data were recorded on a SQUID magnetometer (MPMS Quantum design) in an external magnetic field of 1.0 T. The experimental susceptibility data were corrected for underlying diamagnetism by the use of tabulated Pascal's constants.

X-band EPR spectra were recorded on a Bruker ESP 300 spectrometer. The spectra were simulated by iteration of the (an)isotropic *g* values, hyperfine coupling constants, and line widths. We thank Dr. F. Neese (Abteilung Biologie der Universität Konstanz) for a copy of his EPR simulation program. NMR experiments were carried out on a Bruker ARX 250 (250 and 63 MHz for ^{1}H and ^{13}C NMR, respectively). The internal shift reference for ^{1}H NMR, with CHD_2CN, is δ_H = 1.94. The internal shift reference for ^{13}C NMR, with CD_3CN, is δ_C = 118.3. Abbreviations used are the following: s = singlet; d = doublet; t = triplet.

X-ray Crystallographic Data Collection and Refinement of the Structures. A colorless single crystal of **I**, dark green crystals of **3** and **5**, and black specimens of **2** and **4b** were coated with perfluoropolyether, picked up with glass fibers, and mounted on diffractometers equipped with a nitrogen cold stream at 100 K. Graphite-monochromated Mo Kα radiation (λ = 0.710 73 Å) was used. Crystallographic data of the compounds and diffractometer types used are listed in Table 1. Cell constants were obtained from a least-squares fit of the diffraction angles of several thousand strong reflections. Intensity data were corrected for Lorentz and polarization effects. Data sets of **I**, **2**, and **4b** were corrected for absorption using the program SADABS,[14] whereas the intensities of **3** were left uncorrected. Crystal faces of **5** were

(12) (a) Maslovskaya, L. A.; Petrikevich, D. K.; Timoshchuk, V. A.; Shadyro, O. I. *Russ. J. Gen. Chem.* **1996**, *66*, 1842. Translated from: *Zh. Obsh. Khim.* **1996**, *66*, 1893. (b) FRG Patent No. 1 104522, 1959; *Chem. Abstr.* **1962**, *56*, 5887.

(13) Weisman, G. R.; Vachon, D. J.; Johnson, V. B.; Gronbeck, D. A. *J. Chem. Soc., Chem. Commun.* **1987**, 886.

(14) Sheldrick, G. M. *SADABS*; Universität Göttingen: Göttingen, Germany, 1994.

Table 1. Crystallographic Data for **I**, **2**, **3**, **4b**, and **5**

	I	**2**	**3**	**4b**	**5**
formula	$C_{20}H_{27}NO$	$C_{28}H_{44}CuF_6N_4OP$	$C_{40}H_{50}CuN_2O_2$	$C_{40}H_{46}Cl_4N_2NiO_2$	$C_{40}H_{50}N_2O_2Pd$
fw	297.43	661.18	654.36	787.30	697.22
cryst system	monoclinic	monoclinic	triclinic	monoclinic	triclinic
space group	$P2_1/n$	$P2_1$	$P\bar{1}$	$P2_1/c$	$P\bar{1}$
a, Å	14.7814(14)	9.5859(8)	5.8395(12)	12.1419(9)	5.8007(9)
b, Å	13.3137(12)	11.1967(12)	11.632(2)	10.2848(6)	11.690(2)
c, Å	18.746(2)	15.2022(14)	13.691(2)	15.3145(12)	13.689(2)
α, deg	90	90	109.78(3)	90	108.76(2)
β, deg	103.73(2)	105.69(2)	92.66(3)	92.54(2)	92.80(2)
γ, deg	90	90	94.68(3)	90	94.39(2)
V, Å	3583.7(6)	1570.9(3)	869.5(3)	1910.6(2)	873.7(2)
Z	8	2	1	2	1
T, K	100(2)	100(2)	100(2)	100(2)	100(2)
R1^a [$I > 2\sigma(I)$]	0.0666	0.0445	0.0609	0.0413	0.0506
wR2^b [$I > 2\sigma(I)$]	0.1675	0.0800	0.1502	0.0986	0.1041

^{a} $R1 = \Sigma||F_o| - |F_c||/\Sigma|F_o|$. ^{b} $wR2 = [\Sigma[w(F_o^2 - F_c^2)^2]/\Sigma[w(F_o^2)^2]]^{1/2}$, where $w = 1/\sigma^2(F_o^2) + (aP)^2 + bP$ and $P = (F_o^2 + 2F_c^2)/3$.

determined, and the face-indexed correction routine embedded in ShelXTL[15] was used to account for absorption. The Siemens ShelXTL[15] software package was used for solution, refinement, and artwork of the structures, and neutral atom scattering factors of the program were used. All structures were solved and refined by direct methods and difference Fourier techniques. Non-hydrogen atoms were refined anisotropically, and hydrogen atoms were placed at calculated positions and refined as riding atoms with isotropic displacement parameters. A split atom model with two different orientations and occupation factors of 0.66 and 0.34 was used to model the disorder of the PF_6^- anion in crystals of **2**. Two crystallographically independent molecules are present in the unit cell of **I**. A *tert*-butyl group was found to be disordered in each molecule, and a split model with occupation factors of 0.73:0.27 and 0.60:0.40 was applied, respectively. In addition, one of the molecules shows disorder of the phenol oxygen stemming from a rotation of the phenol by 180° around the N(27)−C(28) bond. The two resulting positions were refined with occupation factors of 0.70 and 0.30.
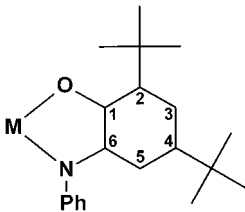
Results

Preparation and Characterization of Complexes. The ligands **I** and **II** are readily available in good yields from the reaction of 3,5-di-*tert*-butylcatechol and aniline or 3,5-dichloroaniline (1:1) in *n*-heptane in the presence of air and the base triethylamine.[12]

The complexes prepared are summarized in Scheme 1. Their synthesis is straightforward. Reaction of **I** with anhydrous $CoCl_2$ (ratio 3:1) in CH_3CN in the presence of NEt_3 and air as oxidant produces deep brown crystals of $[Co^{III}(L^{ISQ})_3]$ (**1**), the crystal structure of which has been reported.[16] Compound **1** is paramagnetic; it has an $S = {}^3/_2$ ground state and contains a low-spin cobalt(III) ion, d^6, and three O,N-coordinated iminobenzosemiquinonato(1−) radical anions, which are intramolecularly ferromagnetically coupled.

From the reaction mixture of $CuCl_2 \cdot 6H_2O$, 1,4-dimethyl-1,4,7-triazacyclononane, and the ligand **I** (ratio 1:1:1) in methanol in the presence of air complex **2**, $[Cu^{II}(dmtacn)(L^{ISQ})]$-$PF_6$, was obtained as dark green crystals. Compound **2** possesses an $S = 1$ ground state (see below).

The reaction of **I** or **II** with salts such as CuCl, $Ni(NO_3)_2 \cdot 6H_2O$, or $PdCl_2$ (ratio 2:1) in CH_3CN or CH_3OH in the presence of air affords dark blue-green crystalline materials of $[Cu(L^{ISQ})_2]$ (**3**), $[Ni(L^{ISQ})_2]$ (**4a**), $[Ni(^{Cl}L^{ISQ})_2]$ (**4b**), and $[Pd(L^{ISQ})_2]$ (**5**), respectively. As we will show below, **3** possesses an $S = {}^1/_2$ ground state whereas **4a** (**4b**) and **5** are diamagnetic. The latter

(15) ShelXTL V.5, Siemens Analytical X-ray Instruments, Inc., 1994.
(16) Verani, C. N.; Gallert, S.; Bill, E.; Weyhermüller, T.; Wieghardt, K.; Chaudhuri, P. *Chem. Commun.* **1999**, 1747.

Table 2. Selected Bond Distances (Å) and Angles (deg)

complex	**2**	**3**	**4b**	**5**	ligand **I**
M−O1	1.935(2)	1.912(2)	1.827(1)	1.977(3)	
M−N1	2.209(3)				
M−N2	2.032(3)				
M−N3	2.066(3)				
M−N4	1.973(2)	1.936(2)	1.859(2)	1.959(3)	
O−C1	1.301(3)	1.290(4)	1.333(3)	1.314(5)	1.376(3)
N−C6	1.343(4)	1.335(4)	1.370(3)	1.352(6)	1.432(3)
C1−C2	1.434(4)	1.436(5)	1.429(3)	1.430(6)	1.405(3)
C2−C3	1.376(4)	1.376(4)	1.396(3)	1.375(6)	1.393(3)
C3−C4	1.428(4)	1.432(5)	1.430(3)	1.431(6)	1.400(3)
C4−C5	1.357(4)	1.369(5)	1.384(3)	1.374(6)	1.387(3)
C5−C6	1.428(4)	1.425(4)	1.430(3)	1.425(6)	1.394(3)
C1−C6	1.442(4)	1.454(5)	1.427(3)	1.430(6)	1.389(3)
N−Ph	1.415(4)	1.416(4)	1.425(3)	1.434(6)	1.410(3)
M−N−C6	111.9(2)	113.0(2)	114.9(1)	114.7(3)	
M−N−Ph	127.2(2)	124.4(2)	124.7(1)	122.4(3)	
C6−N−Ph	120.8(2)	122.4(3)	120.2(2)	122.9(4)	120.9(2)
M−O−C1	113.0(2)	113.2(2)	114.4(1)	113.4(3)	
O−M−N	83.13(9)	83.6(1)	84.6(1)	81.4(1)	

compounds display "normal" ^1H NMR spectra at ambient temperature (see Experimental Section).

Crystal Structures. The crystal structures of the uncoordinated ligand **I** and of the mononuclear complexes **2**, **3**, **4b**, and **5** have been determined by single-crystal X-ray crystallography at 100(2) K. The crystal structure of **1** has been published in a preliminary communication.[16] Figures S1 and S2 display the structures of **5** and of the free ligand **I**, respectively. Table 2 summarizes selected bond distances and angles.

The structure of the free ligand **I** serves as a benchmark for the geometrical details for the fully reduced (i.e. aromatic) form. The six C−C bond distances in the *o*-aminophenol part are observed in the narrow range 1.387(3)−1.405(2) Å (average 1.395 Å) indicating the presence six nearly equidistant aromatic C−C bonds. The average C−C bond distance in the *N*-phenyl ring is 1.385 ± 0.009 Å. The two C−N bonds at 1.432(3) and 1.410(3) Å are typical C−N single bonds, and the C−OH distance at 1.376(3) Å is typical for organic phenols.

The neutral molecule $[Co^{III}(L^{ISQ})_3]$ (**1**) contains three O,N-coordinated *o*-iminobenzosemiquinonato(1−) radical anions

Bis(o-iminobenzosemiquinonato)metal Complexes

J. Am. Chem. Soc., Vol. 123, No. 10, 2001 **2217**
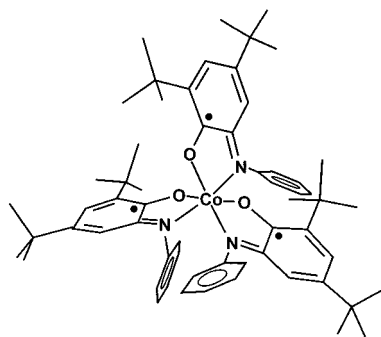
Figure 1. Schematic representation of the neutral molecule [Co^{III}-(L^{ISQ})$_3$] in crystals of **1**.[16]

(L^{ISQ})$^{-}$ [16] as shown in Figure 1. The molecule possesses C_1 symmetry. The metrical details of the three ligands can best be represented by two classical resonance structures E and F. The

E   **F**
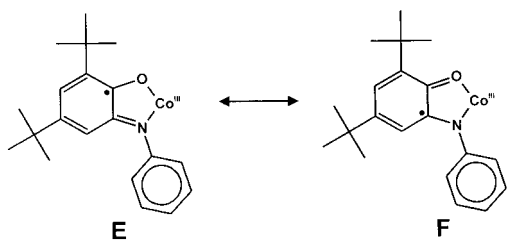
imino C=N bonds at 1.345 ± 0.005 Å are significantly shorter than the C_{phenyl}–N bonds at 1.420 ± 0.005 Å. The average C–O bond distance at 1.304 ± 0.004 Å is also significantly shorter than the 1.35–1.37 Å expected for a coordinated catecholate; it is in the range of those reported for transition metal *o*-benzosemiquinonato(1−) complexes.[5] The six ring C–C distances in the *o*-iminobenzosemiquinonato part are not equidistant, whereas the six C–C distances of the *N*-phenyl part are within experimental error the same at 1.39 ± 0.01 Å. In the *o*-iminobenzosemiquinonate part two alternating relatively short C=C distances are observed at 1.375 ± 0.008 Å in the six-membered ring and four longer C–C bonds at 1.432 ± 0.008. The difference of 0.056 Å between these two average values is larger than our experimental error (±0.009 Å). Therefore, the oxidation level of the ligand (L^{ISQ})$^{-}$ is considered to be correctly represented by the resonance structures E and F.

The most important feature of the structure of **1** is the fact that one electron oxidation of an *o*-aminophenolate to the corresponding iminobenzosemiquinonate leads to characteristic structural changes, which can be readily detected by high-quality X-ray structure determinations. The three equidistant, short Co–O distances at an average 1.888 ± 0.003 Å and the three short Co–N distances at 1.934 + 0.009 Å in **1** are only compatible with a low-spin d^6 configuration of a cobalt(III) ion. Thus in this case an unambiguous assignment of *physical* oxidation states for both the metal ion and the organic radical ligands is achieved.

Crystals of **2** consist of well-separated monocations [Cu^{II}-(dmtacn)(L^{ISQ})]$^{+}$ and PF$_6$ anions. As shown in Figure 2 the copper ion is five-coordinate with a square-based pyramidal coordination polyhedron where the O,N-coordinated ligand, (L^{ISQ})$^{-}$, occupies two basal coordination sites and the macrocycle dmtacn the remaining two. One amine nitrogen is in the fifth apical position. The oxidation level of the ligand (L^{ISQ})$^{-}$ is again unequivocally established as *o*-iminobenzosemiquinonate(1−). As described above for **1**, the short distances C15–N4 at 1.343(4), C16–O1 at 1.301(3), and two C=C distances,
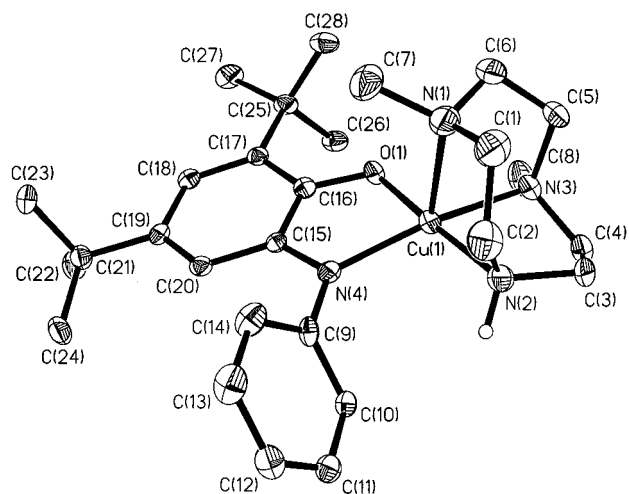
Figure 2. Perspective view of the monocation [Cu^{II}(dmtacn)(L^{ISQ})]$^{+}$ in crystals of **2**. The small open circle represents an amine-hydrogen atom; all other hydrogens are omitted.
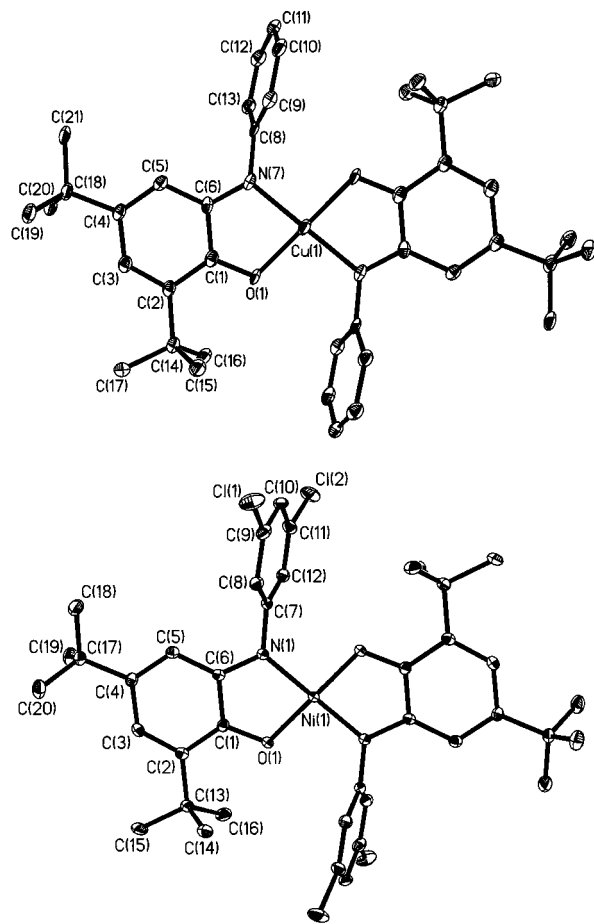

Figure 3. Structures of [Cu^{II}(L^{ISQ})$_2$] (top) and [Ni^{II}($^{Cl}L^{ISQ}$)$_2$] (bottom) in crystals of **3** and **4b**, respectively.

C17–C18 at 1.376(4) and C19–C20 at 1.357(4), contrasting four longer C–C distances C15–C16 1.442(4), C15–C20 1.428(4), C18–C19 1.428(4), and C16–C17 1.434(4) Å, are indicative of a coordinated radical anion.

Crystals of **3**, **4b**, and **5** consist of well-separated neutral molecules [M(L^{ISQ})$_2$] (M = Cu (**3**), Pd (**5**)) and [Ni($^{Cl}L^{ISQ}$)$_2$] in **4b**. Figure 3 shows the structure of [Cu^{II}(L^{ISQ})$_2$] (top) and [Ni^{II}($^{Cl}L^{ISQ}$)$_2$] (bottom); the structure of [Pd(L^{ISQ})$_2$] is displayed in Figure S1. In all three cases the molecules are planar within experimental error. The two nitrogen donor atoms of the two
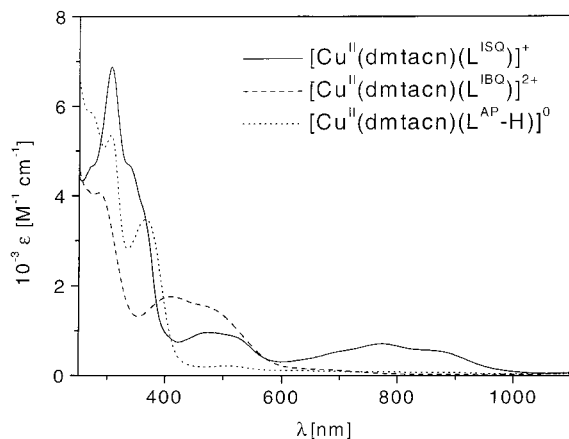
Figure 4. Electronic spectra of [Cu^{II}(dmtacn)(L^{ISQ})]PF$_6$ (**2**) in CH$_2$Cl$_2$ (solid line), its electrochemically generated one-electron oxidized form [Cu^{II}(dmtacn)(L^{IBQ})]$^{2+}$ (dashed line), and its one-electron reduced form [Cu^{II}(dmtacn)(L^{AP}-H)]^0 (dotted line).

(L^{ISQ})$^-$ ligands are always in the trans position with respect to each other (as are the two oxygen donors). The coordination geometry around the nitrogen donor is planar indicating that this nitrogen is three-coordinate (sp^2-hybridization) and not protonated; the same holds for **1** and **2**. The geometrical parameters for the (L^{ISQ})$^-$ or (^{Cl}L^{ISQ})$^-$ ligands are identical to those in **1** and **2** (see Table 2), which again renders the ligands *o*-iminobenzosemiquinonates, and consequently, the metal ions Cu, Ni, and Pd can safely be assigned the physical oxidation state +II.

Magnetochemistry and EPR Spectroscopy. The electronic ground states of complexes **1**−**5** have been established from variable-temperature (3−300 K) magnetic susceptibility measurements by using a SQUID magnetometer.

The magnetic properties of **1** have been reported previously.[16] On lowering of the temperature, μ_{eff} (3.16 μ_B at 290 K) increases monotonically approaching a maximum at ∼15 K with a value of 3.71 μ_B, which is close to the spin-only value for an $S = {}^3/_2$ system expected for the ground state attained from three ferromagnetically coupled iminobenzosemiquinonato radicals. Two exchange coupling constants have to be considered for the simulation based on the Hamiltonian eq 1:

$$H = -2J(S_1 \cdot S_2 + S_2 \cdot S_3) - 2J_{13}(S_1 \cdot S_3) + \sum \mu_B g_i S_i B_i \quad (1)$$

Here $S_1 = S_2 = S_3 = {}^1/_2$. An excellent fit was obtained with $J = J_{12} = J_{23} = +9.1$ cm^{-1} and $J_{13} = +59.5$ cm^{-1}, $g_1^{rad} = g_2^{rad} = g_3^{rad} = 2.005$ (fixed), and TIP = 100 × 10^{-6} cm^3 mol^{-1}. Thus the quartet ground state is separated from the first excited doublet state by 27 cm^{-1}.

Complexes **4a** and **5** possess an $S = 0$ ground state as is clearly shown by the fact that both compounds display ^{1}H NMR spectra without detectable paramagnetic shifts or line broadening of the proton signals even at 298 K.

The temperature dependence of the effective magnetic moment, μ_{eff}, of **2** is shown in Figure 7. In the range 20−120 K a nearly temperature-independent magnetic moment of 2.83 μ_B indicates an $S = 1$ ground state. Above 120 K this moment slowly decreases to 2.77 μ_B at 300 K. This behavior is typical for a spin-coupled system with parallel spin alignment in the ground state and thermal population of excited states with lower spin multiplicities at energies above 200 cm^{-1}. Since the low-temperature value of μ_{eff} is very close to the spin-only value for an isolated $S = 1$ ground state, it is obvious that **2** is a complex containing a Cu^{II} ion ($S_{Cu} = {}^1/_2$) and a ligand radical
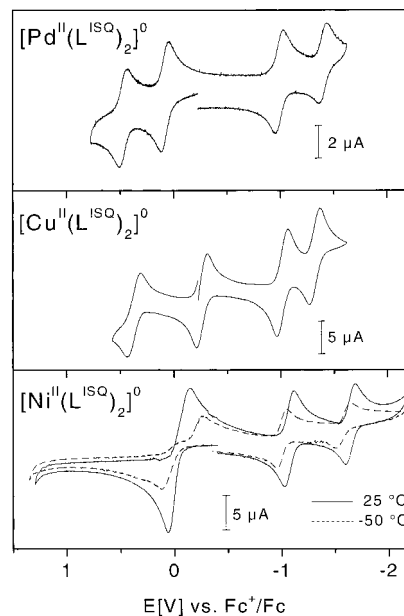

Figure 5. Cyclic voltammograms of **5** (top), **3** (middle), and **4a** (bottom) recorded in CH$_2$Cl$_2$ solutions containing 0.10 [(*n*-Bu)$_4$N]PF$_6$ as supporting electrolyte at a scan rate of 200 mV s^{-1} at 25 °C. (Conditions: glassy carbon electrode; potentials referenced vs the ferrocenium/ferrocene (Fc$^+$/Fc) couple.)

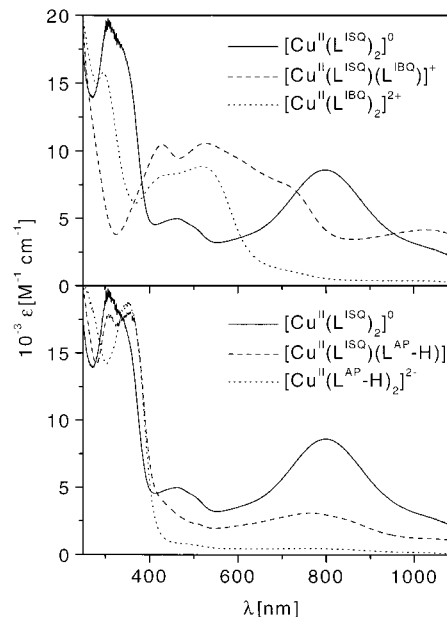**Figure 6.** Electronic spectra of oxidized (top) and reduced (bottom) forms of **3** in CH$_2$Cl$_2$ solutions (0.10 M [(*n*-Bu)$_4$N]PF$_6$).

(L^{ISQ})$^-$ ($S_{rad} = {}^1/_2$), which are intramolecularly ferromagnetically coupled. Accordingly, the magnetic data were readily fitted by using a spin-Hamiltonian model including Heisenberg and Zeeman terms, eq 2. Parameters $J = +195$ cm^{-1}, $g_{Cu} = g_{rad} = 2.0$ (fixed), and $\chi_{TIP} = 60 × 10^{-6}$ cm^3 mol^{-1} are indicative of the strong ferromagnetic coupling between the (d$_{x^2-y^2}$)^1 magnetic orbital at the Cu ion and the π-orbital of the radical (L^{ISQ})$^-$. These two orbitals are strictly orthogonal relative to each other.

$$H = -2J S_{Cu} \cdot S_{rad} + g\mu_B(S_{Cu} + S_{rad}) \cdot B \quad (2)$$

The planar complex **3** also displays a temperature dependence of the effective magnetic moment as shown in Figure 8. At
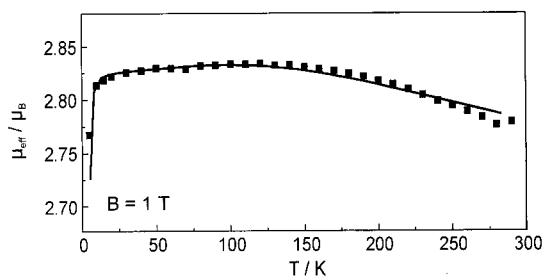
Bis(o-iminobenzosemiquinonato)metal Complexes

J. Am. Chem. Soc., Vol. 123, No. 10, 2001 2219

Figure 7. Temperature dependence of the effective magnetic moment, μ_{eff}, of **2**. Fit parameters are given in the text.
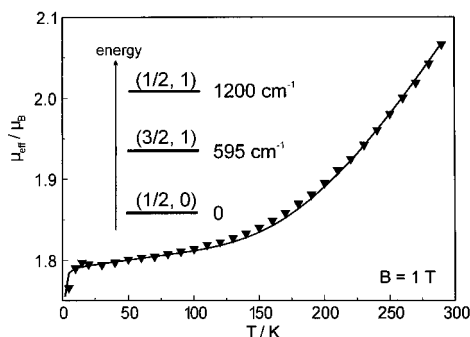

Figure 8. Temperature dependence of the effective magnetic moment, μ_{eff}, of **3**. The inset shows the energetic ordering of the corresponding coupled spin states (S_t, S*) using parameters J and J' given in the text.

temperatures <70 K, a nearly constant value of 1.78 μ_B is indicative of an $S_t = \frac{1}{2}$ ground state. With increasing temperature (>70 K) μ_{eff} increases monotonically indicating thermal population of excited states with *higher* spin multiplicity than 2. This behavior immediately rules out the description of the electronic structure of **3** by two resonance hybrids as shown in structure **D**, i.e., [Cu$^{\text{II}}$(L$^{\text{AP}}$-H)(L$^{\text{IBQ}}$)] ↔ [Cu$^{\text{II}}$(L$^{\text{IBQ}}$)(L$^{\text{AP}}$-H)].

Obviously, **3** is a "multispin" system. Since the ground state is $S_t = \frac{1}{2}$, it must be a three-spin molecule. Such a system possesses three coupled states provided that exchange is the dominating spin interaction. The states are labeled by their total spin $S_t = S_{\text{Cu}} + S_{\text{rad1}} + S_{\text{rad2}}$ and a pair subspin $S^* = S_{\text{rad1}} + S_{\text{rad2}}$, $(S_t, S^*) = (\frac{3}{2}, 1)$, $(\frac{1}{2}, 1)$, and $(\frac{1}{2}, 0)$, or, in a more symbolic fashion, by (↑↑↑), (↑↓↑), and (↑↑↓), respectively. In a symmetric coupling scheme for the planar molecule in **3** with two independent coupling constants the energies of the coupled states are given by $E(\frac{3}{2}, 1) = -J - 2J'$, $E(\frac{1}{2}, 1) = 2(J - J')$, and $E(\frac{1}{2}, 0) = 0$. J describes the coupling between a radical (L$^{\text{ISQ}}$)$^-$ and an adjacent copper(II) ion whereas J' describes that between two remote radical anions. Hence, the relative order of these states depends critically on the values of J and J'.

Intuitively, one might expect antiferromagnetic coupling between the *adjacent* Cu$^{\text{II}}$ and (L$^{\text{ISQ}}$)$^-$ spins leading to an $(\frac{1}{2}, 1)$ ground state (↑↓↑). In fact, the observed magnetic data can be satisfactorily simulated with a single J_{AF} coupling constant. Only the relative energy of the two $S_t = \frac{1}{2}$ states remains rather undetermined since their contributions to μ_{eff} are virtually the same. However, as we will show below EPR spectroscopy conclusively rules out an $(\frac{1}{2}, 1)$ ground state for **3** but establishes an $(\frac{1}{2}, 0)$ ground state (↑↑↓). This then requires *strong* (dominating) antiferromagnetic coupling between the two remote radical anions in **3**.

With this constraint from EPR spectroscopy new simulations of the magnetic data were carried out. Since the energy of the $(\frac{1}{2}, 1)$ excited state turns out to be above that of the multiplet $(\frac{3}{2}, 1)$, the $(\frac{1}{2}, 1)$ state is not populated in the temperature range employed (3−300 K). Therefore, a unique solution for

the two coupling constants, J and J', cannot be found without introducing a further constraint.

Since we have established a strong ferromagnetic spin interaction between a Cu$^{\text{II}}$ ion and an adjacent radical anion in complex **2**, we assume that the same ferromagnetic coupling operates in **3**. This is reasonable, since in both compounds the $(d_{x^2-y^2})^1$ magnetic orbital and that of the π-radical are orthogonal with respect to each other and the Cu(L$^{\text{ISQ}}$) units in both complexes are isostructural. Simulation of the magnetic data of **3** by using a J value of $+195$ cm^{-1} (fixed) yields a strong antiferromagnetic coupling constant, J', of -400 cm^{-1} for the coupling between the two remote radical anions in **3**. The resulting energetic order of states is displayed in the inset of Figure 8. We do not claim that the values for J and J' derived above for **3** represent an unique solution, but in a qualitative fashion the results do demonstrate that spin coupling between a central Cu$^{\text{II}}$ ion and a terminal ligand radical is ferromagnetic and coupling between two remote radical anions is strongly antiferromagnetic.

The nature of the spin ground state of **3** can be sensitively probed by X-band EPR spectroscopy. This is possible because Cu$^{\text{II}}$ (d^9) ions exhibit significant g anisotropy and large hyperfine splittings contrasting in this respect the coordinated organic radical anions. Thus the Cu$^{\text{II}}$ spin serves as an effective reporter spin, which probes the wave function of the coupled system.

The contributions of the Cu$^{\text{II}}$ single ion properties to the coupled spin multiplets depend on the projection of the Cu$^{\text{II}}$ local spin on the respective total spin. Since the Cu$^{\text{II}}$ spin, S_{Cu}, is *antiparallel* to the total spin for the state $(\frac{1}{2}, 1)$ (↑↓↑) and *parallel* for $(\frac{1}{2}, 0)$ (↑↑↓), the "inherited" anisotropic g values (and $^{63/65}$Cu A values) are ordered $g_{\parallel} > g_{\perp}$ for $(\frac{1}{2}, 0)$, like the Cu$^{\text{II}}$ intrinsic values, but $g_{\parallel} < g_{\perp}$ for $(\frac{1}{2}, 1)$. The experimental spectrum of **3** shown in Figure 9 clearly establishes $g_{\parallel} > g_{\perp}$, and consequently, a $(\frac{1}{2}, 0)$ (↑↑↓) ground-state prevails in **3** with dominating antiferromagnetic coupling between the remote radical anions.

The EPR spectrum of **3** in CH$_2$Cl$_2$ solution shown in Figure 9A exhibits axial g values with slight rhombic distortions and $^{63/65}$Cu hyperfine splittings close to values expected for single-ion Cu$^{\text{II}}$ complexes with a $(d_{x^2-y^2})^1$ magnetic orbital. Since we do not know the exact wave function of the ground state doublet, $(\frac{1}{2}, 0)$, due to possible mixing with $(\frac{1}{2}, 1)$ (and probably also with $(\frac{3}{2}, 1)$, if anisotropic or antisymmetric exchange prevails), we refrain from converting the experimental EPR parameters to local ones. It would appear that the dominating radical−radical interaction leads to an almost "isolated" Cu$^{\text{II}}$ spin character of the ground multiplet.

The EPR spectrum of **3** measured in tetrahydrofuran (THF) solution (Figure 9B) is similar but not identical to that of **3** in CH$_2$Cl$_2$. THF is a weak ligand and might coordinate in an apical position forming a square pyramidal species [Cu$^{\text{II}}$(L$^{\text{ISQ}}$)$_2$(THF)]. Interestingly, the spectrum shows a distinct ligand hyperfine splitting which is barely resolved for the $g_{\parallel}$ lines but clearly so at g_x and g_y. A satisfactory simulation was obtained with two equivalent ^{14}N nuclei ($I = 1$) with $A_N = (12, 12, 23) \times 10^{-4}$ cm^{-1}. This anisotropy is presumably due to spin-dipolar contributions of S_{Cu}(!) with spin density mainly in the d$_{x^2-y^2}$ orbital.

Electro- and Spectroelectrochemistry. Cyclic voltammograms (CV) of all complexes have been recorded in CH$_2$Cl$_2$ solutions containing 0.10 M [N(n-Bu)$_4$]PF$_6$ as supporting electrolyte at a glassy carbon working electrode and a Ag/AgNO$_3$ reference electrode. Ferrocene was used as an internal
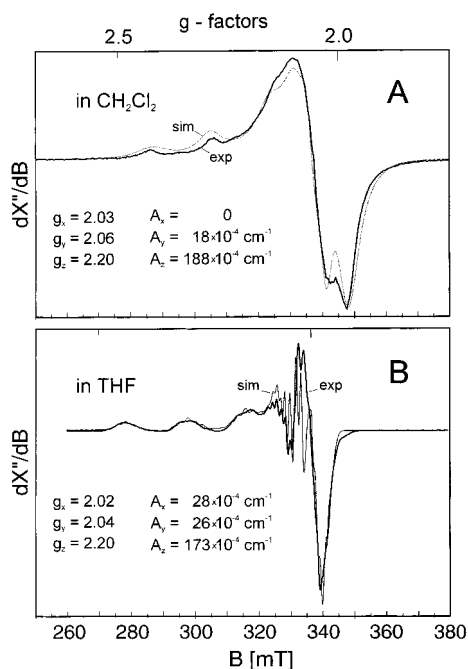
Figure 9. X-band EPR spectra of **3** dissolved in CH$_2$Cl$_2$, A, and tetrahydrofuran, B. Experimental conditions: microwave frequency 9.6539 GHz (A), 9.4389 GHz (B); power 10 μW (A), 1 mW (B); modulation 1 mT (A), 0.4 mT (B) (100 kHz); T = 30 K. The dashed lines are simulations for an effective spin $S = \frac{1}{2}$ with g values and Cu hyperfine parameters as indicated. In (B) an additional ligand hyperfine interaction with two equivalent nitrogen nuclei was considered according to $A_N = (12, 12, 23) \times 10^{-4}$ cm^{-1}. The anisotropic (Gaussian) line widths were $\Gamma = (0.5, 0.5, 1.0)$ T. A-strain contribution to the line widths was also considered by using parameters $C_{2,z} = 3$ for $^{63/65}$Cu and $C_2 = (6, 3, 0)$ for ^{14}N.
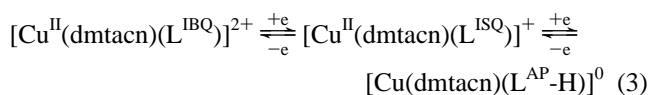
Table 3. Summary of Redox Potentials in Volts vs Ferrocenium/Ferrocene (Fc$^+$/Fc)^a

complex	$E_{1/2}$, V vs Fc$^+$/Fc				
1^a	0.20		−0.35	−0.98	−1.31
2	−0.06		−0.77		
3	0.37		−0.26	−1.02	−1.32
4a		0.042^b		−1.07	−1.64
5	0.47		0.08	−0.99	−1.40

^{a} Conditions: CH$_2$Cl$_2$ solution containing 0.10 M [(n-Bu)$_4$N]PF$_6$; glassy carbon electrode, scan rate 200 mV s^{-1} at 298 K. ^{b} 2e process at 25 °C (200 mV s^{-1} scan rate); see text.

standard, and potentials are referenced versus the ferrocenium/ferrocene couple (Fc$^+$/Fc). Table 3 summarizes the results.
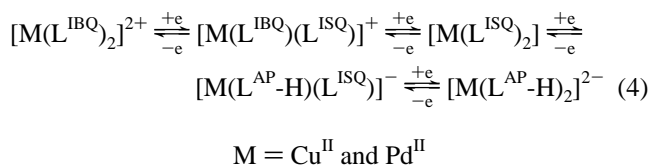
Figure S3 shows the CV of **2** recorded in the potential range +0.3 to −1.0 V. Two reversible one-electron-transfer waves are observed. Coulometric measurements established that the first at $E_{1/2} = -0.06$ V corresponds to a one-electron oxidation of **1** whereas the second at −0.77 V is a one-electron reduction. Spectroelectrochemical measurements shown in Figure 4 prove that both processes are ligand-centered as in eq 3.

$$[Cu^{II}(dmtacn)(L^{IBQ})]^{2+} \underset{-e}{\overset{+e}{\rightleftharpoons}} [Cu^{II}(dmtacn)(L^{ISQ})]^+ \underset{-e}{\overset{+e}{\rightleftharpoons}}$$

$$[Cu(dmtacn)(L^{AP}\text{-}H)]^0 \quad (3)$$

The electronic spectra of these three species (Table S4) allow the characterization of a single O,N-coordinated (L^{IBQ})^0, (L^{ISQ})$^-$, and (L^{AP}-H)$^{2-}$, respectively. The fully reduced form (L^{AP}-H)$^{2-}$ does not have absorption maxima > 600 with intensities >500 M^{-1} cm^{-1}, whereas the coordinated radical anion (L^{ISQ})$^-$ displays four maxima in the range 450−900 nm with relatively
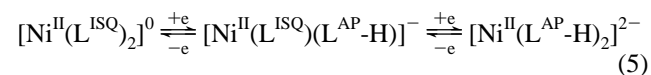
small intensity, ϵ < 1000 M^{-1} cm^{-1}, and the fully oxidized form (L^{IBQ})^0 displays only two intense maxima at 410 and 478 nm (ϵ > 1.5 × 10^3) above 350 nm. These maxima have been observed in the spectrum of the uncoordinated iminobenzoquinone, (L^{IBQ})^0, in CH$_2$Cl$_2$ at 488 nm (ϵ = 2.7 × 10^3 M^{-1} cm^{-1}) as a shoulder and at 396 (4.8 × 10^3) (see Experimental Section). The d−d transitions in the visible of the five-coordinate Cu^{II} ion are significantly less intense ($\epsilon \sim$ 100−500 M^{-1} cm^{-1}); they have not been identified.

The CVs of **3** and **5** are very similar and are displayed in Figure 5. In both cases, four reversible one-electron-transfer waves are observed of which, according to coulometric measurements, two correspond to reductions and two to oxidations. Since the redox potentials are similar irrespective of the nature of the central metal ion (copper or palladium) we assign these processes as ligand centered, eq 4.

$$[M(L^{IBQ})_2]^{2+} \underset{-e}{\overset{+e}{\rightleftharpoons}} [M(L^{IBQ})(L^{ISQ})]^+ \underset{-e}{\overset{+e}{\rightleftharpoons}} [M(L^{ISQ})_2] \underset{-e}{\overset{+e}{\rightleftharpoons}}$$

$$[M(L^{AP}\text{-}H)(L^{ISQ})]^- \underset{-e}{\overset{+e}{\rightleftharpoons}} [M(L^{AP}\text{-}H)_2]^{2-} \quad (4)$$

$$M = Cu^{II} \text{ and } Pd^{II}$$

These assignments are nicely corroborated by the electronic spectra of the electrochemically generated oxidized and reduced forms of **3** and **5**, respectively. Figure 6 displays these spectra of the copper complexes; Figure S4 shows similar results for **5**. The spectra of the dianions [M^{II}(L^{AP}-H)$_2$]$^{2-}$ and of the dications [M^{II}(L^{IBQ})$_2$]$^{2+}$ are very similar to those of [Cu^{II}-(dmtacn)(L^{AP}-H)]^0 and [Cu^{II}(dmtacn)(L^{IBQ})]$^{2+}$ shown in Figure 4. The spectra of the monocations [M^{II}(L^{ISQ})(L^{IBQ})]$^+$ show the presence of both the iminobenzosemiquinonate(1−) and the benzoquinone ligand, whereas the spectra of the monoanions [M^{II}(L^{ISQ})(L^{AP}-H)]$^-$ are a "superposition" of the spectra of (L^{ISQ})$^-$ and (L^{AP}-H)$^{2-}$.

In contrast, the CV of the isostructural nickel complex [Ni^{II}(L^{ISQ})$_2$] (**4a**) is different from those of **3** and **5** in the anodic range (>0 V); see Figure 5. The reduction of **4a** is accomplished by two successive reversible one-electron-transfer waves at $E_{1/2}$ = −1.07 and −1.64 V which closely resemble those in **3** and **5**. Therefore, we assign these reductions as ligand centered processes, eq 5. Spectroelectrochemical investigations of the mono- and dianions confirm this assignment (Figure S5 and Table S4) since these spectra are very similar to those of the corresponding reduced species of **5**.

$$[Ni^{II}(L^{ISQ})_2]^0 \underset{-e}{\overset{+e}{\rightleftharpoons}} [Ni^{II}(L^{ISQ})(L^{AP}\text{-}H)]^- \underset{-e}{\overset{+e}{\rightleftharpoons}} [Ni^{II}(L^{AP}\text{-}H)_2]^{2-}$$
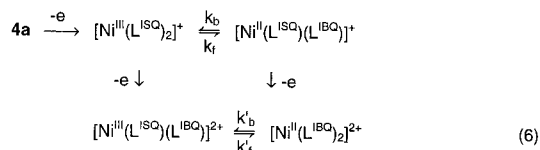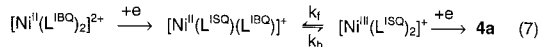$$(5)$$

Controlled-potential coulometry at +0.6 V shows that **4a** can be oxidized by 2 electrons. The resulting dicationic species is stable in solution at −25 °C as is demonstrated by the fact that the UV/vis spectrum as well as the CV recorded of such an oxidized solution after 20 min remain practically unchanged. No chemical decomposition of **4a** or its dication has been detected. Since the electronic spectrum of the dication of **4a** resembles the spectrum of [Pd^{II}(L^{IBQ})$_2$]$^{2+}$, we also assign the iminobenzoquinone oxidation level for the ligands in the dicationic oxidation product of **4a**: [Ni^{II}(L^{IBQ})2]$^{2+}$.

The peak potential separations in the CVs, $\Delta E = E_{p,ox} - E_{p,red}$, observed for the two reduction waves are 90−95 mV which is close to that observed for the ferrocenium/ferrocene couple at a scan rate of 100 mV s^{-1}. In contrast, ΔE for the 2e wave centered at −0.05 V using the same conditions is more than 200 mV at 25 °C and increases markedly to 350 mV at

−50 °C. In addition, ΔE for the 2e oxidation depends strongly on the scan rate whereas ΔE for the 1e reduction waves are constant. After allowance for uncompensated resistance, the anodic and cathodic peak potentials of the 2e process shift with increasing scan rates (30 ± 5 mV to more positive and more negative values, respectively, for each 10-fold increase in scan rate). This behavior suggests that the oxidation is not a simple reversible 2e process but during oxidation and rereduction of **4a** heterogeneous electron transfer steps must be followed by first-order homogeneous reactions. In other words, intermediates must be considered. Note that the first and second scans (without stirring inbetween) yield exactly the same CV. This demonstrates that this redox process represents a chemically fully reversible interconversion of **4a** to its dication (and vice versa) via two intermediates.

These intermediates must involve the central nickel ion since this behavior is not observed for **3** and **5**. It is conceivable (and very likely) that the planar $N_2O_2Ni^{II}$ moiety in **4a** undergoes a metal-centered 1e oxidation yielding a low-spin Ni^{III} ion. The dicationic product, $[Ni^{II}(L^{IBQ})_2]^{2+}$, can then be electrochemically reversibly generated from **4a** by the following ECE mechanism, eqs 6 and 7. By using this scheme the peak positions and their shapes at different scan rates and temperatures can be reasonably well reproduced as is shown in Figure S6. At room temperature

Oxidation:

$$\mathbf{4a} \xrightarrow{-e} [Ni^{III}(L^{ISQ})_2]^+ \underset{k_f}{\overset{k_b}{\rightleftharpoons}} [Ni^{II}(L^{ISQ})(L^{IBQ})]^+$$

$$-e \downarrow \qquad\qquad\qquad \downarrow -e$$

$$[Ni^{III}(L^{ISQ})(L^{IBQ})]^{2+} \underset{k'_f}{\overset{k'_b}{\rightleftharpoons}} [Ni^{II}(L^{IBQ})_2]^{2+} \qquad (6)$$

Reduction:

$$[Ni^{II}(L^{IBQ})_2]^{2+} \xrightarrow{+e} [Ni^{II}(L^{ISQ})(L^{IBQ})]^+ \underset{k_b}{\overset{k_f}{\rightleftharpoons}} [Ni^{III}(L^{ISQ})_2]^+ \xrightarrow{+e} \mathbf{4a} \quad (7)$$

the observed peak positions, $E_{p,ox}$ and $E_{p,red}$, are determined by the two one-electron redox potentials $\mathbf{4a}/[Ni^{III}(L^{ISQ})_2]^+$ ($E^1_{1/2}$) and $[Ni^{II}(L^{IBQ})(L^{ISQ})]^+/[Ni^{II}(L^{IBQ})_2]^{2+}$ ($E^2_{1/2}$), by the equilibrium constant $K = k_f/k_b$, and by the magnitude of k_f and k_b. In addition, the redox couple $[Ni^{III}(L^{ISQ})_2]^+/[Ni^{III}(L^{ISQ})(L^{IBQ})]^{2+}$ ($E^3_{1/2}$) plays also a role at low temperatures (−60 °C) and higher scan rates where the scan rate of the potential increase to reach $E^3_{1/2}$ competes with the rates k_f and k_b of the intramolecular electron transfer. Different combinations of the chemical and electrochemical parameters of the system lead to similar voltammograms. For example, a shift of $E_{1/2}$ by 30 mV and a 10-fold increase of the rate constant of the follow-up reaction have similar effects on the peak positions. Therefore, no unique set of parameters was found which fits the experimental data.

However, a number of constraints must apply: (i) $E^2_{1/2} < E^1_{1/2}$, otherwise the $E_{p,ox}$ and $E_{p,red}$ peaks split into two separate peaks at 25 °C which is not observed. (ii) At 25 °C the equilibrium constant $K = k_f/k_b$ must be in the range 0.1–10 and both individual rates must be fast as compared to the fastest experimental scan rate employed (100 V/s) in order to transfer two electrons without time delay in a single peak. (iii) At −60 °C, however, the kinetics of the adjustment of the equilibrium $K = k_f/k_b$ must be slow enough that at a 1 V/s scan rate a considerable amount of the intermediate $[Ni^{II}(L^{ISQ})(L^{IBQ})]^{2+}$ can form but fast enough that at a scan rate of 0.1 V/s this amount is comparatively small. (iv) It is reasonable to assume that the rate constants k_f, k_b decrease with decreasing temperatures ($\Delta G^‡ \sim$ 15 kcal mol^{-1}). Finally, $E^1_{1/2}$ and $E^2_{1/2}$ should not shift by more than ~80 mV on going from 25 to −60 °C since a shift

Chart 1. Average Bond Distances in the Coordinated Ligands $(L^{ISQ})\bullet^-$ and $(L^{AP})^-$
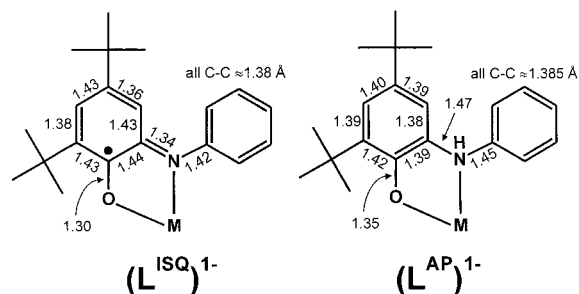
of 1 mV/deg is a typical value for the temperature dependence of reversible 1e redox potentials.

The parameters given in Table S5 satisfactorily simulate the temperature and scan rate dependence of the electrochemical 2e oxidation of **4a**. In view of the numerous constraints this interpretation appears to be quite reliable. We note that we have not been able to simulate the CVs by using an EEC mechanism.

Discussion

High-quality single-crystal X-ray structure determinations at 100 K of complexes **1**–**3**, **4b**, and **5** have allowed us to unambiguously identify the structural characteristics of the O,N-coordinated *o*-iminobenzosemiquinonato(1−) radical. The corresponding 1e-reduced diamagnetic and N-protonated monoanion aminophenolato(1−), $(L^{AP})^-$, has distinctly different geometric parameters. In $[V^V(L^{AP}\text{-}H)_2(L^{AP})]$ both forms of ligand **I** are present and clearly discernible. We will report the structure of this species elsewhere. Chart 1 displays the average C−C, C−N, and C−O distances observed in both forms.

Very similar observations have been made for bidentate *o*-benzosemiquinonato(1−) radicals in crystals of the square planar, diamagnetic complexes $[Ni^{II}(3,6\text{-}SQ)_2]$,[8] $[Pd(3,5\text{-}SQ)_2]$,[10] and $[Pt(3,5\text{-}SQ)_2]$,[10] where the 3,6- and 3,5-di-*tert*-butylbenzo-semiquinonates(1−) are O,O-coordinated to a metal ion. The structures clearly prove the presence of *o*-semiquinonates rather than catecholates or *o*-benzoquinones.

In contrast, only one high-quality crystal structure of an analoguous square planar compound containing the *o*-diimino-benzosemiquinonato(1−) radical, (disq)$^-$, appears to have been reported, namely $[Co^{II}(disq)_2]$.[17] The structure of its nickel analogue,[9] $[Ni^{II}(disq)_2]$, has been reported, but it is of rather low quality. For comparison, compounds containing the *o*-diiminobenzoquinone and the *o*-phenylenediamine ligands have been reported.[18–20] Chart 2 summarizes the structural changes observed.[11] We stress again the importance of high-quality X-ray crystallography for the *experimental* determination of the oxidation level (physical oxidation state) of this class of bidentate noninnocent ligands. This is not so straightforward for the corresponding benzenedithiolato derived series, where the monoanionic radical and its fully oxidized neutral form, the putative 1,2-dithioketone, do not show such marked structural changes. Sellmann et al.[21] have recently reported crystal structures of the series $[Ni(^{bu}S_2)_2]^{2-/1-/0}$, where $^{bu}S_2$ represents the ligand 3,5-*tert*-butyl-*o*-benzenedithiolate(2−).
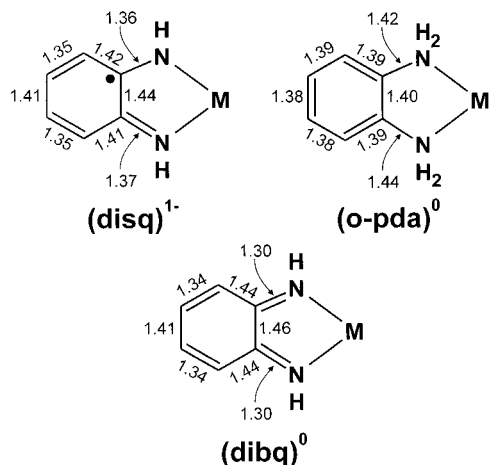
(17) Peng, S.-M.; Chen, C.-T.; Liaw, D.-S.; Chen, C.-I.; Wang, Y. *Inorg. Chim. Acta* **1985**, *101*, L31.
(18) Christoph, G. C.; Goedken, V. L. *J. Am. Chem. Soc.* **1973**, *95*, 3869.
(19) Dickman, M. H. *Acta Crystallogr., Sect. C* **2000**, *C56*, 58.
(20) Cheng, P.-H.; Cheng, H.-Y.; Lin, C.-C.; Peng, S.-M. *Inorg. Chim. Acta* **1990**, *169*, 19.
(21) Sellmann, D.; Binder, H.; Häussinger, D.; Heinemann, F. W.; Sutter, J. *Inorg. Chim. Acta* **2000**, *300*, 829.

Chart 2. Average Bond Distances in the Coordinated (disq)•$^-$, (*o*-pda)^0, and (dibq)^0

Figure 10. Schematic representation of the orientation of three π radical ligands with respect to a filled (or empty) t_{2g} metal orbital in an octahedral complex.

Figure 11. Antiferromagnetic exchange pathway between two π radical ligands and a filled t_{2g} metal orbital in square planar complexes [ML$_2$] (M = Ni^{II}, Pd^{II}, Pt^{II}, Cu^{II}).

Upon coordination of *one* of the above bidentate monoanionic radicals to a paramagnetic transition metal ion as in **2** and the copper(II) complexes [Cu^{II}(Me$_3$-[12]N$_3$)(3,5-SQ)]ClO$_4$[22] (Me$_3$-[12]N$_3$ is 2,4,4-trimethyl-1,5,9-triazacyclodedec-1-ene) and [Cu^{II}(NH$_{py2}$)(3,5-SQ)]ClO$_4$[23] (NH$_{py2}$ is di-2-pyridylamine), the radical spin and the spin of the Cu^{II} ion ($S_{Cu} = \frac{1}{2}$) couple strongly in an intramolecular ferromagnetic fashion due to the orthogonality of the two magnetic orbitals. Consequently, a triplet ground state ($S_t = 1$) is observed in these cases. These results provide direct experimental proof that a ligand radical is coordinated to a paramagnetic Cu^{II} ion.[24−26]

An interesting situation is encountered when *three* radicals are coordinated to a diamagnetic low-spin cobalt(III) ion in an octahedral fashion as in **1** and [Co^{III}(3,6-SQ)$_3$],[24] both of which have been characterized by X-ray crystallography. Interestingly, **1** has an $S_t = \frac{3}{2}$ but [Co^{III}(3,6-SQ)$_3$] possesses an $S_t = \frac{1}{2}$ ground state. Thus intramolecular ferromagnetic and antiferromagnetic coupling is observed for two structurally quite similar complexes. Despite this difference in the ground state the magnetochemistry establishes again unequivocally that in both complexes there are three organic radicals present. As shown in Figure 10, there are at least three antiferromagnetic exchange coupling pathways available in a tris(bidentate chelate)cobalt(III) complex with three π-radical magnetic orbitals. In addition, at least twice as many ferromagnetic pathways are identifiable. Since the sign of the observed coupling constant J is determined by the sum of the anti-, J_{AF}, and ferromagnetic contributions, J_F, it is clear that very subtle structural differences between **1** and [Co^{III}(3,6-SQ)$_3$] determine the multiplicity of their ground states. The measured effective J values for **1** (+59 and +9.5 cm^{-1}) and for [Co(3,6-SQ)$_3$] ($J = -39$ cm^{-1}) are small and close to zero where J_{AF} and J_F nearly cancel. Interestingly, tris(semiquinonato)metal complexes containing a central metal ion with a d^0 electron configuration as in Al(III), Ga(III), and Ti(IV) are found to be ferromagnetically coupled ($S_t = \frac{3}{2}$) but also only weakly so.[24,25,26a]
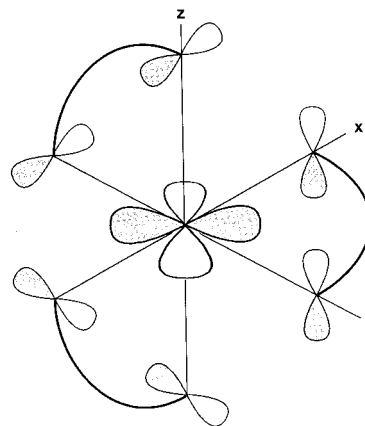
(22) Benelli, C.; Dei, A.; Gatteschi, D.; Pardi, L. *Inorg. Chem.* **1990**, *29*, 3409.

(23) Kahn, O.; Prins, R.; Reedijk, J.; Thompson, J. S. *Inorg. Chem.* **1987**, *26*, 3557.

(24) Lange, C. W.; Couklin, B. J.; Pierpont, C. G. *Inorg. Chem.* **1994**, *33*, 1276.

(25) Adam, D. M.; Rheingold, A. L.; Dei, A.; Hendrickson, D. M. *Angew. Chem., Int. Ed. Engl.* **1993**, *32*, 391.

(26) (a) Bruni, S.; Caneschi, A.; Cariati, F.; Delfs, C.; Dei, A.; Gatteschi, D. *J. Am. Chem. Soc.* **1994**, *116*, 1388 and references therein. (b) Speier, G.; Csihony, J.; Whalen, A. M.; Pierpont, C. G. *Inorg. Chem.* **1996**, *35*, 3519. (c) Ruf, M.; Noll, B. C.; Groner, M. D.; Yee, G. T.; Pierpont, C. G. *Inorg. Chem.* **1997**, *36*, 4860.
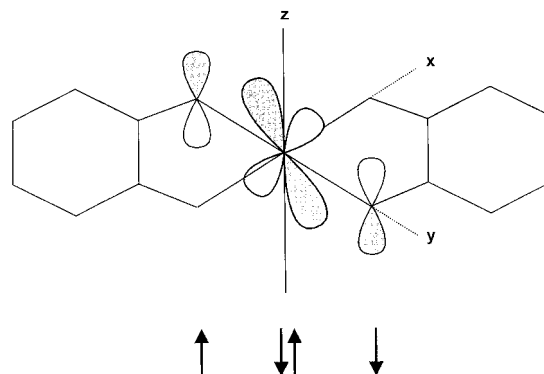
We now turn to the electronic structure of neutral, square planar bis(bidentate chelate)metal complexes [M−N$_4$], [M−N$_2$O$_2$], and [M−O$_4$], where the respective metal ion is Co(II), Ni(II), Cu(II), Pd(II), or Pt(II). As pointed out above, the high-quality crystal structures of [Ni(3,6-SQ)$_2$][8] and [M(3,5-SQ)$_2$] (M = Pd, Pt)[10] have clearly established the presence of two O,O-coordinated *o*-benzosemiquinonato(1−) radicals, and consequently, we can assign a physical oxidation state +II to the respective central metal ion with a d^8 electron configuration. All of these species are diamagnetic even at room temperature. However, Fox and Pierpont[10] have observed temperature-dependent paramagnetic line broadening and shift of the *tert*-butyl ^{1}H NMR resonances of [Pd^{II}(3,5-SQ)$_2$] and have attributed this to the effect of "residual, low-level paramagnetism". For these compounds radical−radical exchange mediated by a filled t_{2g} orbital of the central Ni(II), Pd(II), and Pt(II) as shown in Figure 11 has been invoked. In other words, these compounds are considered to be singlet diradicals with a triplet excited state which is not (or very little) populated at 298 K.

Complexes **3**, **4a,b**, and **5** possess also an $S_t = 0$ ground state. Their crystal structures clearly show the presence of two radicals (L^{ISQ})$^-$. We propose the same electronic structure, namely a singlet diradical, for these complexes.

The most informative compounds with respect to electronic structure are the two copper(II) species **3** and [Cu^{II}(3,6-SQ)$_2$], the crystals of which have been reported to be isomorphous with those of its square planar Ni(II) analogue.[8] Both species possess an $S_t = \frac{1}{2}$ ground state, but at higher temperatures (>100 K) the excited $S_t = \frac{3}{2}$ state is populated, which proves
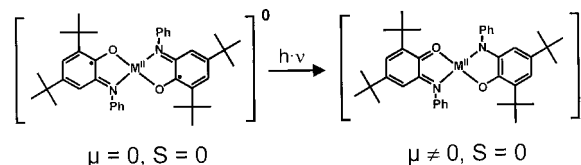
Figure 12. Spin and dipole (μ) allowed transition in [ML$_2$] complexes.

experimentally that these compounds are three-spin systems comprising two organic radical spins and a Cu^{II} d^9 spin.

It was shown above that exchange coupling between a radical and an adjacent Cu(II) ion is strongly ferromagnetic, namely $J_F = +195$ cm^{-1} in **3** and $+100$ cm^{-1} in [Cu^{II}(3,6-SQ)$_2$],[8] but very strongly antiferromagnetic between the two radicals ($J_{AF} = -400$ cm^{-1} in **3** and -179 cm^{-1} in [Cu^{II}(3,6-SQ)$_2$][8]). Thus in the [Cu−O$_4$] species both interactions are about half as effective as those in the [Cu−N$_2$O$_2$] species **3**. A Cu−N bond is expected to be more covalent than a Cu−O bond. If this trend holds for [Cu−N$_4$] complexes, one would expect the unknown [Cu^{II}(disq)$_2$] species to possess a temperature-independent (4− 300 K) magnetic moment of ∼1.73 μ_B (the spin-only value for a Cu(II) ion). The structure of [Co^{II}(disq)$_2$] is known[20] and shows the presence of two diiminobenzosemiquinonato(1−) radicals; its ground state is $S_t = {}^1/_2$ (low-spin d^7).[6]

To summarize the above discussion, we propose that the neutral square planar complexes of the type [M^{II}−N$_4$]^0, [M^{II}−N$_2$O$_2$]^0, and [M^{II}−O$_4$] all contain a divalent transition metal ion (Co, Ni, Pd, Pt, Cu) and two bidentate radical monoanions, which are strongly antiferromagnetically coupled. *The compounds containing a diamagnetic central metal ion with d^8 electron configuration are thus singlet diradicals.*

The electronic spectra of these compounds and of their mono- and dicationic as well as their mono- and dianionic forms are very informative with respect to their electronic structures. The spectra of [Cu^{II}(dmtacn)(L^{ISQ})]$^+$, [Cu^{II}(dmtacn)(L^{IBQ})]$^{2+}$, and [Cu^{II}(dmtacn)(L^{AP}-H)]^0 shown in Figure 4 (Table S4) are dominated by relatively intense π−π* transitions of the respective ligand in the range 300−1100 nm. They are quite distinctive for the oxidation level of the ligand and allow us to discern between (L^{AP}-H)$^-$, (L^{ISQ})$^-$, and (L^{IBQ}). Therefore, it is possible to assign the following oxidation levels in the mono- and dication of **5** as [Pd^{II}(L^{ISQ})(L^{IBQ})]$^+$ and [Pd^{II}(L^{IBQ})$_2$]$^{2+}$, whereas the mono- and dianions are described as [Pd^{II}(L^{ISQ})(L^{AP}-H)]$^-$ and [Pd^{II}(L^{AP}-H)$_2$]$^{2-}$. Similar considerations allow the same assignments of ligand oxidation levels in the redox analogues of **3** and **4a**.[4b]

It is now remarkable that the above spectra do not display the very intense ($\epsilon > 10^4$ M^{-1} cm^{-1}) absorption maximum in the range 750−950 nm which is observed for the neutral complexes **3**, **4a,b**, and **5**. Thus this transition cannot be a π−π* transition of the coordinated (L^{ISQ})$^-$ radical or a ligand-to-metal charge-transfer band. We assign this transition to a spin- and dipole-allowed ligand-to-ligand transition shown in Figure 12. In Table S6 we have compiled the corresponding spectral data for neutral, square planar [M−N$_4$]^0, [M−O$_4$]^0, and [M−S$_4$] complexes all of which have been described as deep blue crystalline materials and all of which display this ligand-to-

Scheme 2. Electronic Structures of Ground and Excited States of Complexes [ML$_2$] (M = Ni, Pd, Pt).
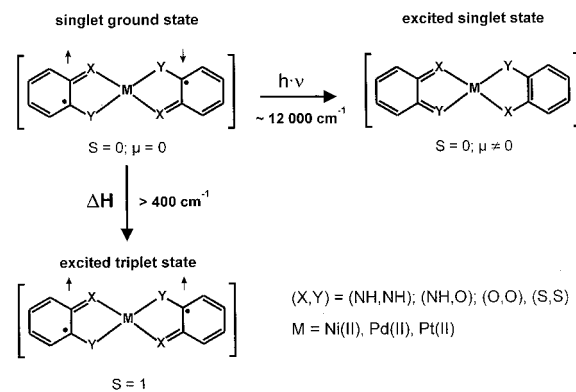
ligand transition in the visible−irrespective of the nature of the central metal ion (Co, Ni, Pd, Pt, or Cu) and the donor atoms (four nitrogens, four oxygens, four sulfurs, or two nitrogens and two oxygens). The above assignment is corroborated by early extended Hückel and multiple-scattering Xα model calculations for [Ni^{II}(disq)$_2$], which also support the singlet diradical description.[27]

Conclusion

We have shown that all neutral, diamagnetic square planar complexes of Ni^{II}, Pd^{II}, and Pt^{II} of the type [M−O$_4$], [M−N$_4$], and [M−O$_2$N$_2$] contain two bidentate O,O-, N,N- and O,N-coordinated *o*-semiquinonato(1−) radical ligands. The two radical spins are intramolecularly, strongly antiferromagnetically coupled giving rise to the observed singlet ground state. Their electronic structures are best described as singlet diradicals. The electronic structures of the ground and excited states of the diamagnetic square planar complexes of Ni^{II}, Pd^{II}, and Pt^{II} containing two semiquinonate(1−) radical ligands can therefore be summarized as shown in Scheme 2.

Supporting Information Available: Figures S1−S6, displaying the structures of **5** and of the ligand **I**, the CV of **2**, the electronic spectra of oxidized and reduced forms of **5** and of **4a**, and the CVs of **4a**, Tables S4−S6, containing electronic spectra of complexes, fit parameters of the CV of **4a**, and a compilation of the ligand-to-ligand CT band in square planar complexes, and additional tables of crystallographic structure refinement data, atom coordinates, bond lengths and angles, anisotropic thermal parameters, and calculated positional parameters of H atoms for **I** and complexes **1**−**3**, **4b**, and **5**. This material is available free of charge via the Internet at http://pubs.acs.org.

(27) Weber, J.; Daul, C.; von Zelewsky, A.; Goursot, A.; Penigault, E. *Chem. Phys. Lett.* **1982**, *88*, 78.